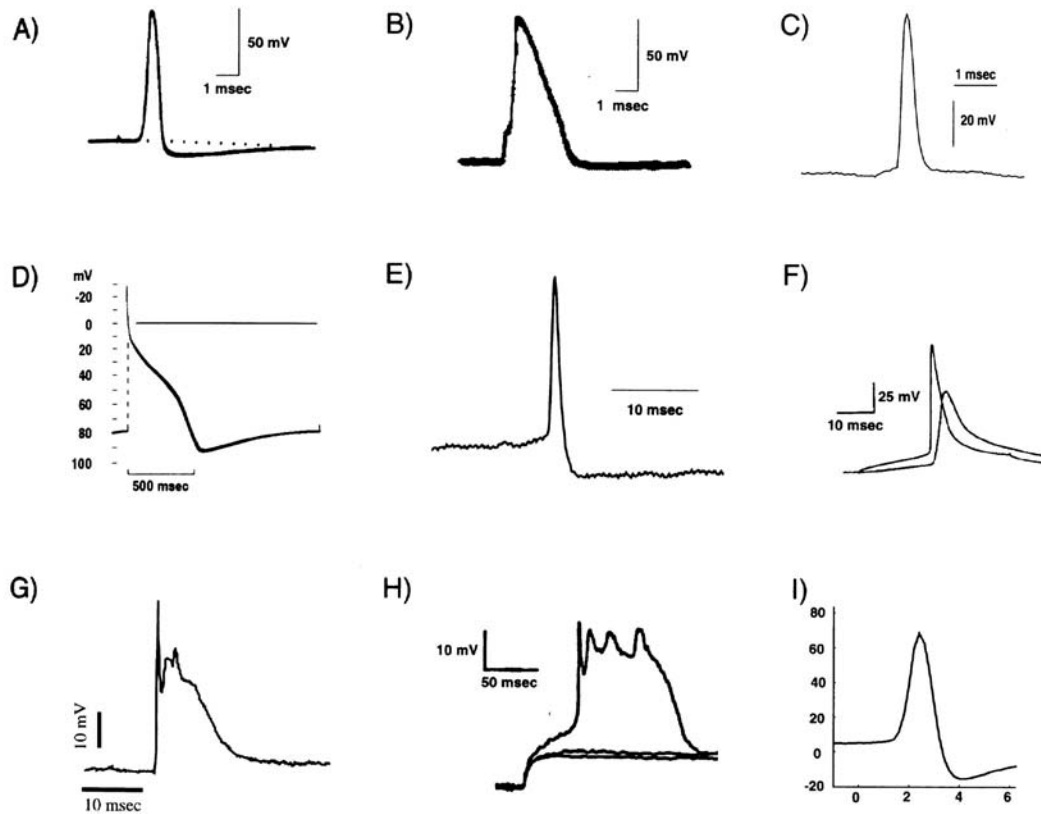


# ECE 796:

# Models of the Neuron

Slides for Lecture #4

Friday, February 2, 2007



**Fig. 6.1 ACTION POTENTIALS OF THE WORLD** Action potentials in different invertebrate and vertebrate preparations. Common to all is a threshold below which no impulse is initiated, and a stereotypical shape that depends only on intrinsic membrane properties and not on the type or the duration of the input. (A) Giant squid axon at 16° C. Reprinted by permission from Baker, Hodgkin, and Shaw (1962). (B) Axonal spike from the node of Ranvier in a myelinated frog fiber at 22° C. Reprinted by permission from Dodge (1963). (C) Cat visual cortex at 37° C. Unpublished data from J. Allison, printed with permission. (D) Sheep heart Purkinje fiber at 10° C. Reprinted by permission from Weidmann (1956). (E) Patch-clamp recording from a rabbit retinal ganglion cell at 37° C. Unpublished data from F. Amthor, printed with permission. (F) Layer 5 pyramidal cell in the rat at room temperatures. Simultaneous recordings from the soma and the apical trunk. Reprinted by permission from Stuart and Sakmann (1994). (G) A complex spike—consisting of a large EPSP superimposed onto a slow dendritic calcium spike and several fast somatic sodium spikes—from a Purkinje cell body in the rat cerebellum at 36° C. Unpublished data from D. Jaeger, printed with permission. (H) Layer 5 pyramidal cell in the rat at room temperature. Three dendritic voltage traces in response to three current steps of different amplitudes reveal the all-or-none character of this slow event. Notice the fast superimposed spikes. Reprinted by permission from Kim and Connors (1993). (I) Cell body of a projection neuron in the antennal lobe in the locust at 23° C. Unpublished data from G. Laurent, printed with permission.

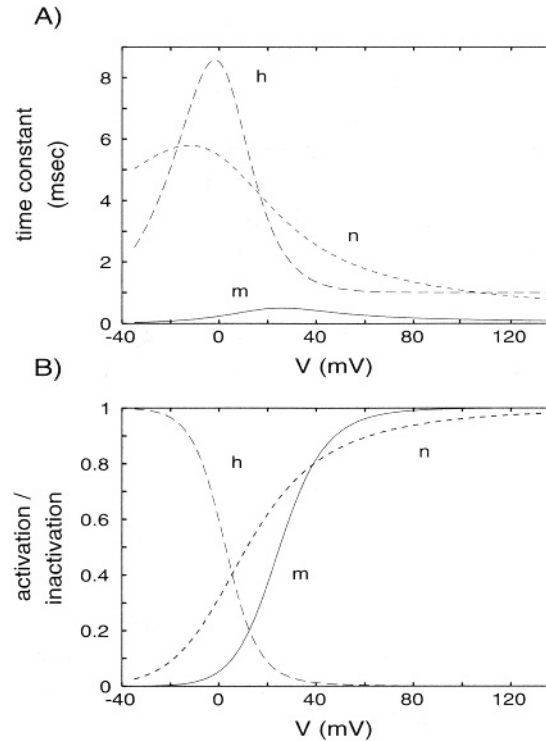


**Fig. 6.3 VOLTAGE DEPENDENCY OF THE GATING PARTICLES** Time constants (A) and steady-state activation and inactivation (B) as a function of the relative membrane potential  $V$  for sodium activation  $m$  (solid line) and inactivation  $h$  (long dashed line) and potassium activation  $n$  (short, dashed line). The steady-state sodium inactivation  $h_{\infty}$  is a monotonically decreasing function of  $V$ , while the activation variables  $n_{\infty}$  and  $m_{\infty}$  increase with the membrane voltage. Activation of the sodium and potassium conductances is a much steeper function of the voltage, due to the power-law relationship between the activation variables and the conductances. Around rest,  $G_{Na}$  increases  $e$ -fold for every 3.9 mV and  $G_K$  for every 4.8 mV. Activating the sodium conductance occurs approximately 10 times faster than inactivating sodium or activating the potassium conductance. The time constants are slowest around the resting potential.

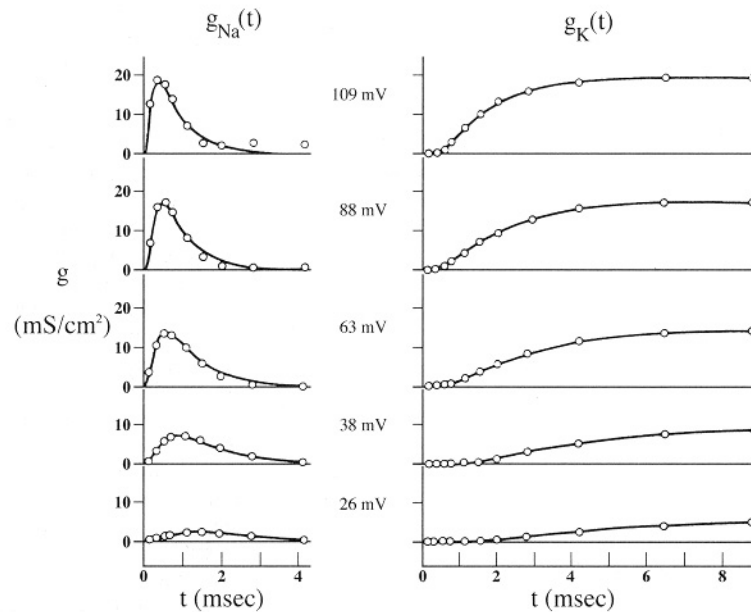


**Fig. 6.4  $K^+$  AND  $Na^+$  CONDUCTANCES DURING A VOLTAGE STEP** Experimentally recorded (circles) and theoretically calculated (smooth curves) changes in  $G_{Na}$  and  $G_K$  in the squid giant axon at  $6.3^\circ C$  during depolarizing voltage steps away from the resting potential (which here, as throughout this chapter, is set to zero). For large voltage changes,  $G_{Na}$  briefly increases before it decays back to zero (due to *inactivation*), while  $G_K$  remains activated. Reprinted by permission from Hodgkin (1958).

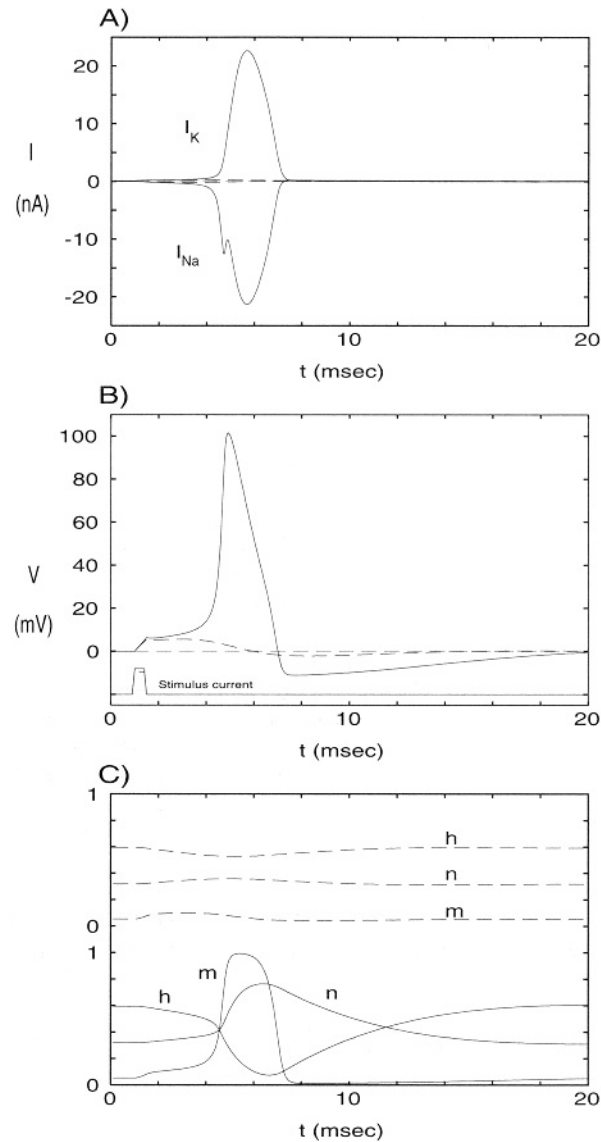


**Fig. 6.5 HODGKIN-HUXLEY ACTION POTENTIAL** Computed action potential in response to a 0.5-msec current pulse of 0.4-nA amplitude (solid lines) compared to a subthreshold response following a 0.35-nA current pulse (dashed lines). **(A)** Time course of the two ionic currents. Note their large sizes compared to the stimulating current. **(B)** Membrane potential in response to threshold and subthreshold stimuli. The injected current charges up the membrane capacity (with an effective membrane time constant  $\tau = 0.85$  msec), enabling sufficient  $I_{Na}$  to be recruited to outweigh the increase in  $I_K$  (due to the increase in driving potential). The smaller current pulse fails to trigger an action potential, but causes a depolarization followed by a small hyperpolarization due to activation of  $I_K$ . **(C)** Dynamics of the gating particles. Sodium activation  $m$  changes much more rapidly than either  $h$  or  $n$ . The long time course of potassium activation  $n$  explains why the membrane potential takes 12 msec after the potential has first dipped below the resting potential to return to baseline level.

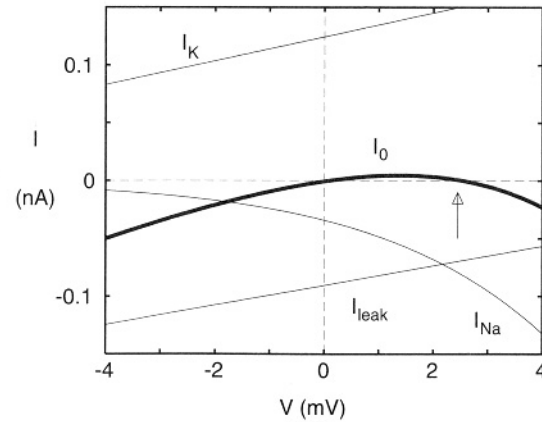


**Fig. 6.6 CURRENT-VOLTAGE RELATIONSHIP AROUND REST** Instantaneous  $I$ - $V$  relationship,  $I_0$ , associated with the standard patch of squid axon membrane and its three components:  $I_0 = I_{Na} + I_K + I_{leak}$  (Eq. 6.21). Because  $m$  changes much faster than either  $h$  or  $n$  for rapid inputs, we computed  $G_{Na}$  and  $G_K$  under the assumption that  $m$  adapts instantaneously to its new value at  $V$ , while  $h$  and  $n$  remain at their resting values.  $I_0$  crosses the voltage axis at two points: a stable point at  $V = 0$  and an unstable one at  $V_{th} \approx 2.5$  mV. Under these idealized conditions, any input that exceeds  $V_{th}$  will lead to a spike. For the “real” equations,  $m$  does not change instantaneously and nor do  $n$  and  $h$  remain stationary; thus,  $I_0$  only crudely predicts the voltage threshold which is, in fact, 6.85 mV for rapid synaptic input. Note that  $I_0$  is specified in absolute terms and scales with the size of the membrane patch.

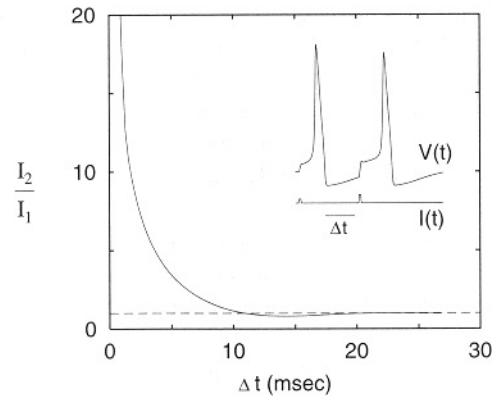


**Fig. 6.7 REFRACTORY PERIOD** A 0.5-msec brief current pulse of  $I_1 = 0.4$  nA amplitude causes an action potential (Fig. 6.5). A second, equally brief pulse of amplitude  $I_2$  is injected  $\Delta t$  msec after the membrane potential due to the first spike having reached  $V = 0$  and is about to hyperpolarize the membrane. For each value of  $\Delta t$ ,  $I_2$  is increased until a second spike is generated (see the inset for  $\Delta t = 10$  msec). The ratio  $I_2/I_1$  of the two pulses is here plotted as a function of  $\Delta t$ . For several milliseconds following repolarization, the membrane is practically inexcitable since such large currents are unphysiological (*absolute refractory period*). Subsequently, a spike can be generated, but it requires a larger current input (*relative refractory period*). This is followed by a brief period of reduced threshold (hyperexcitability). No more interactions are observed beyond about  $\Delta t = 18$  msec.

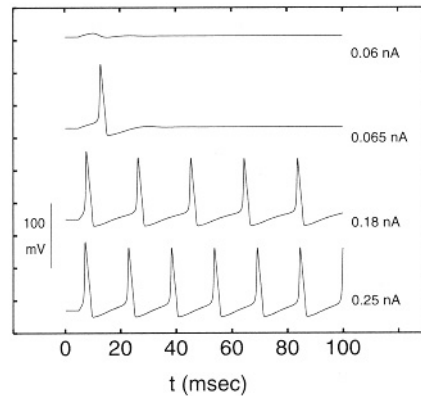


**Fig. 6.8 REPETITIVE SPIKING** Voltage trajectories in response to current steps of various amplitudes in the standard patch of squid axonal membrane. The minimum sustained current necessary to initiate a spike, termed *rheobase*, is 0.065 nA. In order for the membrane to spike indefinitely, larger currents must be used. Experimentally, the squid axon usually stops firing after a few seconds due to secondary inactivation processes not modeled by the Hodgkin-Huxley equations (1952d).

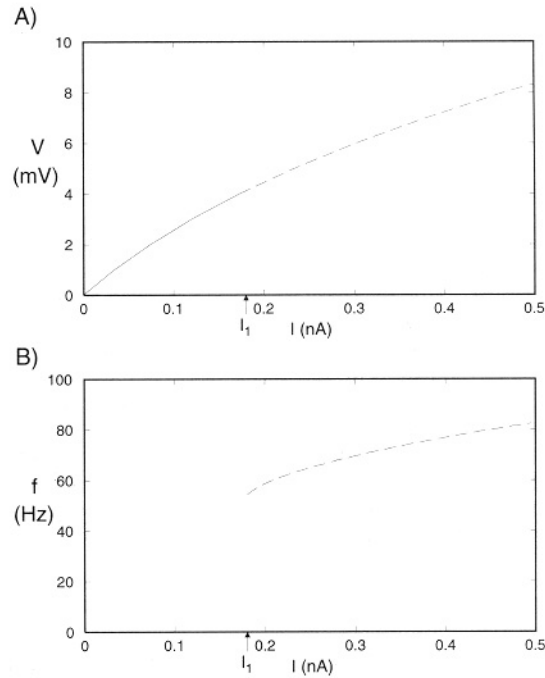


**Fig. 6.9 SUSTAINED SPIKING IN THE HODGKIN-HUXLEY EQUATIONS** (A) Steady-state  $I-V$  relationship and (B)  $f-I$  or discharge curve as a function of the amplitude of the sustained current  $I$  associated with the Hodgkin-Huxley equations for a patch of squid axonal membrane. For currents less than 0.18 nA, the membrane responds by a sustained depolarization (solid curve). At  $I_1$ , the system loses its stability and generates an infinite train of action potentials: it moves along a stable limit cycle (dashed line). A characteristic feature of the squid membrane is its abrupt onset of firing with nonzero oscillation frequency. The steady-state  $I-V$  curve can also be viewed as the sum of all steady-state ionic currents flowing at any particular membrane potential  $V_m$ .



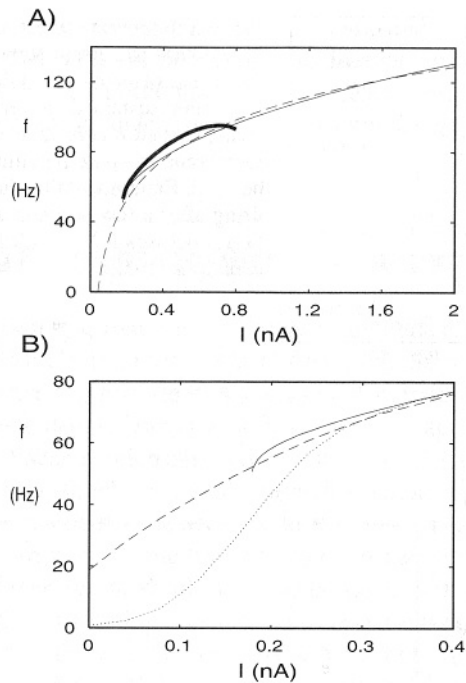


**Fig. 6.10 HODGKIN-HUXLEY  $f-I$  CURVE AND NOISE** (A) Relationship between the amplitude of an injected current step and the frequency of the resultant sustained discharge of action potentials ( $f-I$  curve) for a membrane patch of squid axon at 6.3° C (solid line) and its numerical fit (dashed line) by  $f = 33.2 \log I + 106$ . Superimposed in bold is the  $f-I$  curve for the standard squid axon cable (using normalized current). Notice the very limited bandwidth of axonal firing. (B)  $f-I$  curve for the membrane patch case around its threshold (rheobase) in the presence of noise. White (2000-Hz band-limited) current noise whose amplitude is Gaussian distributed with zero mean current is added to the current stimulus. In the absence of any noise (solid line) the  $f-I$  curve shows abrupt onset of spiking. The effect of noise (dotted curve—standard deviation of 0.05 nA; dashed curve—0.1 nA) is to linearize the threshold behavior and to increase the bandwidth of transmission (stochastic linearization). Linear  $f-I$  curves are also obtained when replacing the continuous and deterministic Hodgkin-Huxley currents by discrete and stochastic channels (see Sec. 8.3).